EKSAKTA
Journal of Sciences and Data Analysis

E-ISSN: 2720-9326
P-ISSN: 2716-0459
DOI : 10.20885/EKSAKTA.vol6.iss1.art5

Temporal and Spatial Analysis of Vegetation and Non-Vegetation Using Landsat 8 Imagery with a Support Vector Machine Approach

Syifa Fauziyah[1], Achmad Fauzan[2,*]

[1,2] Department of Statistics, Faculty of Mathematics and Natural Sciences, Universitas Islam Indonesia, Jl. Kaliurang km. 14,5 Sleman, Yogyakarta 55584 Indonesia.
[*] *Corresponding author: achmadfauzan@uii.ac.id*

Received:14 January 2025; Accepted:15 April 2025; Published:30 April 2025

Abstract: Kertajati International Airport is one of the newest airports located in Majalengka regency, West Java province. The establishment of this airport has sparked interest as a case study, particularly regarding land-use changes around the Kertajati area and, more broadly, in Majalengka Regency. This study aims to measure the extent of changes in vegetated and non-vegetated land around Kertajati International Airport, Majalengka Regency, West Java Province. The methodology employed involves the Support Vector Machine (SVM) classification method. Various kernels, including (1) linear, (2) polynomial, (3) radial basis function (RBF), and (4) sigmoid, were simulated in the analysis. The data used in this study comprise Landsat 8 satellite imagery obtained from Google Earth Engine, utilizing bands such as red, green, blue, near-infrared (NIR), and shortwave infrared (SWIR) for the years 2013 and 2023. The dataset was split using the hold-out method into four scenarios, with varying training and testing data proportions: 75%-25%, 80%-20%, 85%-15%, and 90%-10%. Each scenario was repeated 40 times to ensure robust results. The best results were achieved using the SVM model with an RBF kernel at a data split ratio of 75%-25%, as indicated by the highest accuracy scores. Consistent with the accuracy, the evaluation metrics also fell into a high-performance category. Land area predictions for the vicinity of Kertajati International Airport were analyzed based on the optimal data split proportion. The results of this study reveal a significant reduction in vegetated land from 2013 to 2023, accompanied by a notable increase in non-vegetated land over the same period.

Keywords: Landsat 8, Land Use Changes, Satellite Imagery, Support Vector Machine.

Introduction

Land use represents the result of human activities aimed at fulfilling needs and ensuring sustainable living, which continues to evolve over time. As time progresses, spatial planning and land use management must be regulated to create environments that are more efficient, sustainable, and functional. Land management includes urban planning and infrastructure development, such as roads, railways, bridges, airports, and other transportation networks [1]. In Indonesia, particularly on the island of Java, land use has undergone significant changes across various sectors, including agriculture, settlements, industry, and transportation. Infrastructure changes, such as the construction of roads, airports, and seaports, play a crucial role in driving economic development [2]. However, rapid changes also pose challenges to environmental sustainability and economic growth, as diverse land uses often require careful planning to mitigate potential negative impacts [3].

In West Java, Majalengka Regency has become a key location for infrastructure development due to the presence of Kertajati International Airport, one of the largest projects in the region. Officially inaugurated on June 8, 2018, and fully operational by October 2023, the airport's strategic location in Kertajati District was chosen to support international air traffic. The development of Kertajati Airport has significantly influenced infrastructure development in the surrounding areas, including the construction of roads to provide access for the community and create better connectivity [4].In addition to road development, the

E-ISSN: 2720-9326
P-ISSN: 2716-0459
DOI : 10.20885/EKSAKTA.vol6.iss1.art5

airport has also spurred the construction of supporting facilities such as hotels, restaurants, and shopping centers around its vicinity. However, such developments can potentially have an impact on the local community and environment, highlighting the importance of proper planning and management to minimize negative consequences on the surrounding areas [5].

Changes in infrastructure over time are essential for planning purposes, enabling the government to execute better strategies and avoid resource wastage. Support Vector Machine (SVM) is a classification method that can be utilized to categorize data into specific groups based on patterns and characteristics present in the dataset [6]. This method offers several advantages, including: (1) effectiveness in handling high-dimensional data [7], (2) flexibility through the use of various kernels [8], (3) relatively fast computational processes [9], and (4) applicability across diverse domains [10]. Several studies have successfully implemented the SVM method in various fields, such as diabetic retinopathy detection [11], cardiac detection [12], land quality classification [13], cybersecurity [14], text classification [15], and many others. These applications demonstrate the versatility and robustness of SVM as a tool for solving complex classification problems.

In relation to these infrastructure changes, one alternative approach that can be undertaken is through satellite imagery analysis. Landsat 8 data is a type of satellite imagery used to observe the Earth's surface with medium spatial resolution. This imagery provides information across various electromagnetic spectra, including bands sensitive to visible light, near-infrared, and thermal infrared [16], [17]. Based on these characteristics, the utilization of this imagery combined with the application of the SVM method offers a robust approach to monitoring and evaluating land cover changes in areas with significant potential for transformation, such as the vicinity of Kertajati International Airport in Majalengka Regency, West Java Province.

Materials and Methods

Materials

The study focuses on the area surrounding Kertajati International Airport in Majalengka Regency, West Java Province, from 2013 to 2023. The research sample consists of vegetation and non-vegetation data, selected using the purposive sampling method with the condition that each class is adequately represented. The data utilized in this study is Landsat 8 satellite imagery obtained from Google Earth Engine. The variables in this study are categorized into three types: location variables, dependent variables, and independent variables. The location variables include the x (easting) variable, representing longitude coordinates, and the y (northing) variable, representing latitude coordinates. These location variables serve as markers for the observed objects but are not included in the classification process. The dependent variable consists of vegetation and non-vegetation objects. Meanwhile, the independent variables are derived from the bands of Landsat 8 satellite imagery. The independent variables used in this study include the red, green, blue, near-infrared (NIR), and shortwave infrared (SWIR) bands.

Methods

The study begins with the acquisition of Landsat 8 satellite imagery. The data source is obtained from Google Earth Engine, covering the years 2013 to 2023. The dataset consists of seven variables, including location and predictor variables derived from spectral bands (blue, green, red, NIR, and SWIR). The predictor variables are used to provide information for distinguishing between forests, agricultural land, settlements, and water bodies. As shown in Table 1, the dataset comprises 176,063 pixels, each with a spatial resolution of 10 meters. The research workflow is illustrated in Figure 1. As depicted in Figure 1, after acquiring satellite imagery, digitization was performed by distributing 20,000 points for each category, resulting in a total of 40,000 points for modeling. The digitization process and the acquisition of satellite imagery are not necessarily sequential. Digitization can be conducted prior to or after acquiring the satellite imagery, as long as the boundaries of the study area are clearly defined. Subsequently, each point was merged with the corresponding spectral band variables, as illustrated in Figure 2.

Figure 2 illustrates the merging process of satellite imagery data with digitization results, consisting of 16 pixels (4 x 4 grid). Each square represents one pixel unit from the satellite imagery, with specific

E-ISSN: 2720-9326
P-ISSN: 2716-0459
DOI : 10.20885/EKSAKTA.vol6.iss1.art5

coordinates corresponding to its location. Figure 2(a) illustrates the satellite imagery bands, comprising five spectral bands. Figure 2(b) depicts the data classes acquired from digitization. Certain pixels belong to specific classes, indicated as V (Vegetation) and NV (Non-Vegetation). Pixels marked with "?" represent undigitized pixels, with their classes to be determined through prediction. Figure 2(c) combines the satellite imagery band data (Figure 2(a)) and the digitization results (Figure 2(b)). This illustration highlights how satellite imagery and digitization data are integrated to facilitate further analysis.

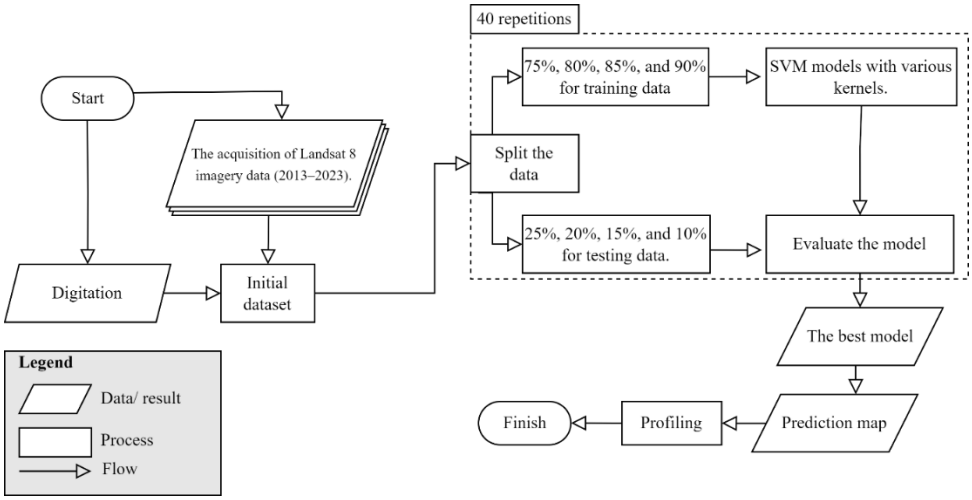

Figure 1. Research Stages (Source: Researcher's Documentation)

Blue band			
2	1	8	4
6	8	3	1
5	3	9	9
1	4	1	2

Green band			
3	6	5	2
7	9	0	1
7	3	8	2
6	2	1	8

Red band			
0	2	4	8
7	3	7	3
4	1	9	5
1	9	6	8

NIR band			
1	2	8	7
4	6	3	9
2	3	5	8
9	6	0	7

SWIR band			
9	4	0	8
2	8	3	4
5	3	1	7
1	6	1	3

(a)

Class			
NV	V	NV	?
V	?	V	NV
V	V	NV	NV
NV	?	?	V

(b)

Combine			
23019 NV	16224 V	85480 NV	?
67742 V	?	30733 V	11394 NV
57425 V	33133 V	98951 NV	92587 NV
16191 NV	?	?	28873 V

(c)

Figure 2. Illustration of Merging Bands with Random Points: (a) Band values, (b) Digitization results, (c) Integration of band values and digitization results (Source: Researcher's Documentation).

From the obtained dataset, the next step involves splitting the data using the Hold-Out method, dividing it into training and testing datasets. Four scenarios were implemented to achieve optimal results, with varying proportions of training and testing data as follows: 75%:25%, 80%:20%, 85%:15%, and 90%:10%. Parameter tuning was performed iteratively using a trial-and-error approach to ensure optimal performance of the classification model. Each scenario was repeated 40 times to ensure the data distribution fell within the theoretically defined interval, avoiding significant fluctuations in the evaluation metrics. This iterative process was conducted to maintain the stability and reliability of the classification results. In each scenario, classification was performed using the Support Vector Machine (SVM) method. SVM is a widely popular machine learning technique for classification and regression tasks. Developed by Boser, Guyon, and

E-ISSN: 2720-9326
P-ISSN: 2716-0459
DOI : 10.20885/EKSAKTA.vol6.iss1.art5

Vapnik, SVM aims to identify a hyperplane that maximally separates two distinct classes with the largest margin [18]. One of the primary advantages of SVM is its ability to handle non-linear data through the use of kernels. Kernels allow SVM to map data from a lower-dimensional space to a higher-dimensional space without requiring explicit transformations, enabling the separation of patterns that are not linearly separable in the original feature space [19], [20]. The kernels utilized in this study include SVM Kernel Linear, SVM Kernel Polynomial, SVM Kernel Radial Basis Function (RBF), and SVM Kernel Sigmoid. The mathematical formulations for each kernel are presented in Table 1.

Table 1. Types of SVM Kernels [20]

No	SVM Kernels	Fungsi Kernel	Information
1.	Linear	$K(x, x_i) = x_i^T x$	x represents the feature vector used for training or prediction, while x_i denotes the feature vector of the i-th observation. The linear kernel is the simplest type of kernel, representing the dot product between two feature vectors. It is commonly used when the data is linearly separable, as it directly calculates the similarity between data points in the original feature space.
2.	Radial Basis Function (RBF)	$K(x, x_i) = \exp(-\gamma\|x - x_i\|^2)$	The parameter γ controls the influence of a single data point. A smaller γ value allows a data point to have a broader influence, while a larger γ value restricts the influence to a narrower region. The RBF kernel maps data into an infinite-dimensional feature space, enabling the separation of complex, non-linear patterns in the data.
3.	Polynomial	$K(x, x_i) = (1 + x \cdot x_i^T)^d$	d is degree of kernel function.
4.	Sigmoid	$K(x, x_i) = \tanh(\gamma . x_i x + r)$	The parameter γ controls the slope of the activation function (tanh), while r adjusts its shift. These parameters work together to shape the decision boundary, allowing it to better adapt to the data and capture complex patterns effectively.

The margin is defined as the distance between the hyperplane and the nearest data points from each class [21]. The hyperplane serves as a separator, which can be a straight line or a flat plane that divides the classes [22]. An illustration of the hyperplane search process is presented in Figure 3.

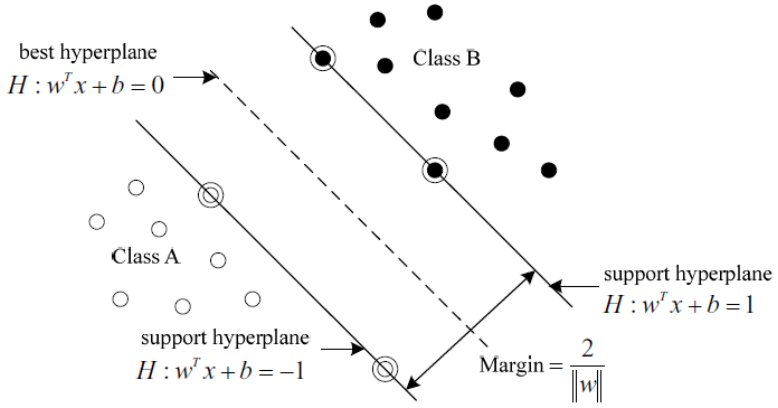

Figure 3 Hyperplane Illustration (source: Sun, 2013 [23])

E-ISSN: 2720-9326
P-ISSN: 2716-0459
DOI : 10.20885/EKSAKTA.vol6.iss1.art5

Based on Figure 3, the pattern illustrates the presence of two classes: negative and positive. The optimal hyperplane is determined by maximizing the margin and identifying the closest points to the hyperplane, known as support vectors. The optimal hyperplane is positioned equidistantly between the positive and negative hyperplanes, represented by the dashed line [24]. SVM offers several advantages, including high accuracy, low error rates, and the ability to address overfitting. Furthermore, SVM efficiently computes distances using support vectors, resulting in faster computational processes. However, despite its advantages, SVM has limitations, particularly its difficulty in handling datasets with large sample sizes and high-dimensional features [25]. For each scenario and its iterations, evaluation metrics were calculated using accuracy, sensitivity, specificity, F1-score, and Area Under Curve (AUC). The calculations for each evaluation metric are presented in Equations (1–5) [26], [27].

$$\text{accuracy} = \frac{\text{TP}}{\text{TP} + \text{TN} + \text{FP} + \text{FN}} \tag{1}$$

$$\text{sensitivity} = \frac{\text{TP}}{\text{TP} + \text{FN}} \tag{2}$$

$$\text{Specificity} = \frac{\text{TN}}{\text{TN+FP}} \tag{3}$$

$$\text{f1} - \text{score} = 2 \cdot \frac{\text{precision} \cdot \text{recall}}{\text{precision} + \text{recall}} \tag{4}$$

$$\text{AUC} = \int_0^1 \text{TPR}\, \text{d(FPR)} \tag{5}$$

True Positive Rate (TPR) and False Positive Rate (FPR) are key metrics for evaluating classification performance. The values of TPR and FPR are defined in Equations (6) and (7), respectively.

$$\text{TPR} = \frac{\text{TP}}{\text{TP} + \text{FN}} \tag{6}$$

$$\text{FPR} = \frac{\text{FP}}{\text{FP} + \text{TN}} \tag{7}$$

True Positive (TP), False Positive (FP), True Negative (TN), and False Negative (FN) represent the four fundamental components of classification evaluation. These values are derived from the confusion matrix, a table used to assess the performance of a classification model by comparing the predicted outcomes with the actual values [28]. Predictions for the entire area surrounding Kertajati International Airport were performed after the best model was identified. Using this model, predictions were made for each year from 2013 to 2023. Once annual results were obtained, the extent of changes in vegetated and non-vegetated land was calculated for each area and time period. These results provide an overview of the magnitude of changes within each class over the specified period.

Results and Discussion

Intial Dataset

Based on the flowchart, the first step involves creating the initial dataset by merging random point data with band data. The visualization of the random point distribution is presented in Figure 4.

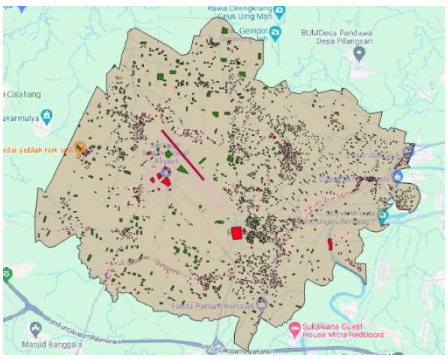

E-ISSN: 2720-9326
P-ISSN: 2716-0459
DOI : 10.20885/EKSAKTA.vol6.iss1.art5

(a) (b)

Figure 4. (a) Point Distribution, (b) Digitization Illustration (source: Processed Data).

Figure 4 shows the distribution of points used in the analysis. Red points represent objects categorized as non-vegetation, while green points indicate objects categorized as vegetation. In real-world contexts, examples of objects in the vegetation category include rice fields, forests, and gardens. Conversely, objects in the non-vegetation category include buildings, vacant land, highways, and pedestrian roads. From Figure 4, the point distribution can also be presented in tabular form, as shown in Table 2.

Table 2. Illustration of the Research Dataset

No	X (mS)	Y (mN)	Blue band	Green band	Red band	NIR band	SWIR band	class
1	185437.5	9264705	0.12146	0.11370	0.10036	0.32418	0.21986	0
2	185440.5	9264721	0.12123	0.11380	0.09848	0.32717	0.23080	0
⋮	⋮	⋮	⋮	⋮	⋮	⋮	⋮	⋮
39999	184292.4	9262063	0.13289	0.11774	0.11542	0.23608	0.21924	1
40000	184301.2	9262059	0.13289	0.11774	0.11542	0.23608	0.21924	1

Table 2 illustrates the research dataset used for classification modeling with the SVM method. In the class column, a value of 0 represents the vegetation class, while a value of 1 represents the non-vegetation class. Data splitting was conducted using four scenarios, with varying proportions of training and testing data: 75%:25%, 80%:20%, 85%:15%, and 90%:10%. Each scenario was repeated 40 times to ensure the results were robust and not merely coincidental. During the preprocessing stage, several steps were performed on the satellite imagery data to ensure it was ready for analysis. These steps included geometric correction, atmospheric correction, study area clipping, and cloud masking. These corrections are essential to maintain the accuracy and quality of the extracted information [29].

SVM Classification

The next step involves classification using SVM with various kernels. Table 3 presents the evaluation metrics values for the training data using the SVM method with a linear kernel under different proportions. Meanwhile, Table 4 provides the evaluation metrics values for the testing data.

Table 3. Illustration of Simulation of Training Data Proportion

simulation	Proportion (%)	Accuracy	Sensitivity	Specificity	f1-score	AUC	Error Rate
1	75 : 25	0.8541	0.8840	0.8285	0.8482	0.8541	0.1459
2	75 : 25	0.8523	0.8798	0.8285	0.8468	0.8523	0.1477
⋮	⋮	⋮	⋮	⋮	⋮	⋮	⋮
40	75 : 25	0.8532	0.8824	0.8281	0.8474	0.8532	0.1468
41	80 : 20	0.8536	0.8827	0.8286	0.8478	0.8536	0.1464
42	80 : 20	0.8528	0.8820	0.8277	0.8469	0.8528	0.1472
⋮	⋮	⋮	⋮	⋮	⋮	⋮	⋮
80	80 : 20	0.8547	0.8830	0.8303	0.8491	0.8547	0.1453
81	85 : 15	0.8537	0.8829	0.8286	0.8479	0.8537	0.1463
82	85 : 15	0.8522	0.8822	0.8266	0.8462	0.8522	0.1478
⋮	⋮	⋮	⋮	⋮	⋮	⋮	⋮
120	85 : 15	0.8541	0.8828	0.8294	0.8484	0.8541	0.1459
121	90 : 10	0.8539	0.8825	0.8293	0.8482	0.8539	0.1461
122	90 : 10	0.8531	0.8816	0.8286	0.8474	0.8531	0.1469

E-ISSN: 2720-9326
P-ISSN: 2716-0459
DOI : 10.20885/EKSAKTA.vol6.iss1.art5

simulation	Proportion (%)	Accuracy	Sensitivity	Specificity	f1-score	AUC	Error Rate
⋮	⋮	⋮	⋮	⋮	⋮	⋮	⋮
160	90 : 10	0.8529	0.8823	0.8276	0.8470	0.8529	0.1471

Table 4. Illustration of Simulation of Testing Data Proportion

Simulation	Proportion (%)	Accuracy	Sensitivity	Specificity	f1-score	AUC	Error Rate
1	75 : 25	0.8516	0.8802	0.8270	0.8458	0.8516	0.1484
2	75 : 25	0.8552	0.8873	0.8280	0.8489	0.8552	0.1448
⋮	⋮	⋮	⋮	⋮	⋮	⋮	⋮
40	75 : 25	0.8532	0.8846	0.8266	0.8470	0.8532	0.1468
41	80 : 20	0.8536	0.8827	0.8286	0.8478	0.8536	0.1464
42	80 : 20	0.8528	0.8820	0.8277	0.8469	0.8528	0.1472
⋮	⋮	⋮	⋮	⋮	⋮	⋮	⋮
80	80 : 20	0.8547	0.8830	0.8303	0.8491	0.8547	0.1453
81	85 : 15	0.8537	0.8829	0.8286	0.8479	0.8537	0.1463
⋮	⋮	⋮	⋮	⋮	⋮	⋮	⋮
120	85 : 15	0.8541	0.8828	0.8294	0.8484	0.8541	0.1459
121	90 : 10	0.8539	0.8825	0.8293	0.8482	0.8539	0.1461
⋮	⋮	⋮	⋮	⋮	⋮	⋮	⋮
160	90 : 10	0.8529	0.8823	0.8276	0.8470	0.8529	0.1471

Similar calculations were also performed for polynomial, RBF, and sigmoid kernels. For each scenario, statistical summaries were provided, focusing particularly on the mean values of each evaluation metric. A summary of the average evaluation metrics for each proportion is presented in Table 5.

Table 5. Mean Values of Evaluation Metrics for Each Scenario

SVM Kernels	Evaluation Metrics	75% : 25%		80% : 20%		85% : 15%		90% : 10%	
		Training (%)	Testing (%)	Trainin g (%)	Testin g (%)	Training (%)	Testing (%)	Training (%)	Testin g (%)
Linear	Accuracy	85.34	85.27	85.33	85.31	85.34	85.29	85.35	85.20
	Sensitivicy	88.24	88.36	88.25	88.34	88.25	88.34	88.23	88.35
	Specificity	82.85	82.65	82.83	82.73	82.85	82.68	82.87	82.54
	f1_Score	84.76	84.66	84.75	84.71	84.77	84.67	84.77	84.57
	AUC	85.34	85.27	85.33	85.31	85.34	85.29	85.35	85.20
	Error Rate	14.66	14.73	14.67	14.69	14.66	14.72	14.65	14.80
Polynomial	Accuracy	84.98	84.57	84.96	84.46	85.03	84.27	84.98	84.15
	Sensitivicy	90.19	90.76	90.18	90.67	90.17	90.83	90.16	91.12
	Specificity	83.94	83.30	83.92	83.17	84.00	82.89	83.95	82.67
	f1_Score	80.97	80.03	80.95	79.92	81.05	79.55	80.99	79.26
	AUC	84.98	84.57	84.96	84.46	85.03	84.27	84.98	84.15
	Error Rate	15.02	15.43	15.04	15.54	14.97	15.73	15.02	15.85
RBF	Accuracy	86.78	86.59	86.78	86.56	86.78	86.51	86.80	86.46
	Sensitivicy	90.68	90.60	90.70	90.51	90.70	90.40	90.72	90.35
	Specificity	86.11	85.89	86.11	85.87	86.11	85.83	86.13	85.77
	f1_Score	83.56	83.30	83.55	83.32	83.55	83.31	83.57	83.26
	AUC	86.78	86.59	86.78	86.56	86.78	86.51	86.80	86.46
	Error Rate	13.22	13.41	13.22	13.44	13.22	13.49	13.20	13.54

E-ISSN: 2720-9326
P-ISSN: 2716-0459
DOI : 10.20885/EKSAKTA.vol6.iss1.art5

SVM Kernels	Evaluation Metrics	75% : 25%		80% : 20%		85% : 15%		90% : 10%	
		Training (%)	Testing (%)	Training (%)	Testing (%)	Training (%)	Testing (%)	Training (%)	Testing (%)
Sigmoid	Accuracy	67.99	67.93	67.97	68.14	67.95	68.06	67.95	68.10
	Sensitivicy	68.00	67.93	67.98	68.15	67.95	68.07	67.95	68.13
	Specificity	67.99	67.92	67.97	68.13	67.95	68.05	67.94	68.07
	f1_Score	67.99	67.92	67.97	68.13	67.95	68.05	67.94	68.06
	AUC	67.99	67.93	67.97	68.14	67.95	68.06	67.95	68.10
	Error Rate	67.99	67.93	67.97	68.14	67.95	68.06	67.95	68.10

Based on Table 5, the SVM method with an RBF kernel was selected to predict the land area surrounding Kertajati International Airport from 2013 to 2023. The illustration of the prediction results is presented in Figure 5. Figure 5(a) presents a raster visualization of the study area. Vegetation objects are represented in black, while non-vegetation objects are represented in white. Figure 5(b) provides a magnified illustration of the classification results, where vegetation is shown in red and non-vegetation in white. These color choices were made to facilitate easier interpretation of the results. The next step involves calculating the proportional area of each class around Kertajati International Airport using a buffering analysis. Buffers with radii ranging from one to nine kilometers from the airport's center were created to compute the area of each class.

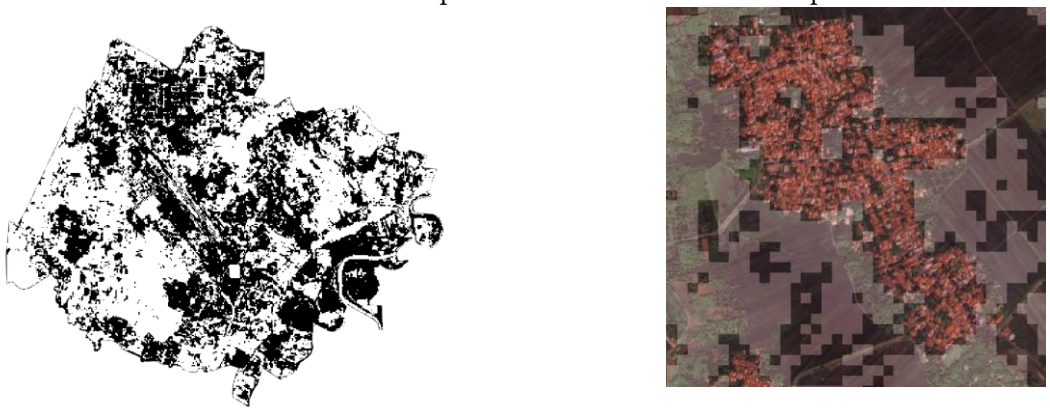

Figure 5 Visualization of Prediction Results, (a) Land classification around Kertajati International Airport, (b) Magnified illustration of the classification results. (source: Processed Data)

Table 6 presents the area of vegetation corresponding to each radius from the center of Kertajati International Airport.

Table 6. Vegetation Buffering Analysis

Year	Radius (m)								
	1000	2000	3000	4000	5000	6000	7000	8000	9000
2013	75.18	70.76	72.52	73.41	74.45	76.21	77.1	77.56	77.56
2014	33.6	42.72	53.85	59.87	62.67	66.05	67.31	68.05	68.13
2015	73.78	69.54	67.05	64.67	64.87	67.94	69.79	70.5	70.54
2016	61.01	66.2	76.08	79.9	81.34	82.79	83.29	83.33	83.18
2017	44.56	60.06	69.62	68.31	69.97	72.57	74.04	74.53	74.51
2018	60.66	63.66	66.76	68.88	69.19	70.65	71.73	72.02	71.85
2019	68.47	76.89	78.92	78.16	77.15	77.22	77.38	77.21	77.01
2020	56.72	65.28	72.24	73.71	74.39	75.84	77.01	77.36	77.29
2021	65.76	73.01	78.78	79.16	79.01	80.02	80.61	80.59	80.39
2022	72.15	73.47	79.01	79.91	80.36	81.41	81.97	82	81.86
2023	52.32	56.23	57.69	57.08	56.62	58.96	60.1	60.5	60.43

E-ISSN: 2720-9326
P-ISSN: 2716-0459
DOI : 10.20885/EKSAKTA.vol6.iss1.art5

Based on Table 6, the buffering analysis of vegetation data reveals that the values for each radius exhibit random variations over certain time periods. However, some radii display consistent changes over time compared to others. Radius 1–3 km: This range shows greater variation, accompanied by a sharp decline in vegetation area from 2013 to 2023. Radius 4–6 km: the values in this range tend to be more stable, with noticeable increases observed in 2016 and 2019. Radius 7–9 km: this range displays consistently stable and higher values, particularly in 2019 and 2022. Following this analysis, the total area of each class surrounding the airport was calculated for every year. The percentage of area for each class over the 11-year period is presented in Table 7.

Table 7. Percentage of Vegetation and Non-Vegetation

No	Year	Percentage of Vegetation	Percentage of Nonvegetation
1.	2013	74.97%	25.03%
2.	2014	58.03%	41.97%
3.	2015	68.74%	31.26%
4.	2016	77.46%	22.54%
5.	2017	67.57%	32.43%
6.	2018	68.38%	31.62%
7.	2019	76.49%	23.51%
8.	2020	72.20%	27.80%
9.	2021	77.48%	22.52%
10.	2022	79.13%	20.87%
11.	2023	57.77%	42.23%

Based on Table 7, the observed random variations over certain time periods may be attributed to various factors, including economic conditions and weather patterns. However, in general, a decline in vegetation class can be observed over the 11-year period. An example of land cover changes from 2013 to 2023 is illustrated in Figure 6.

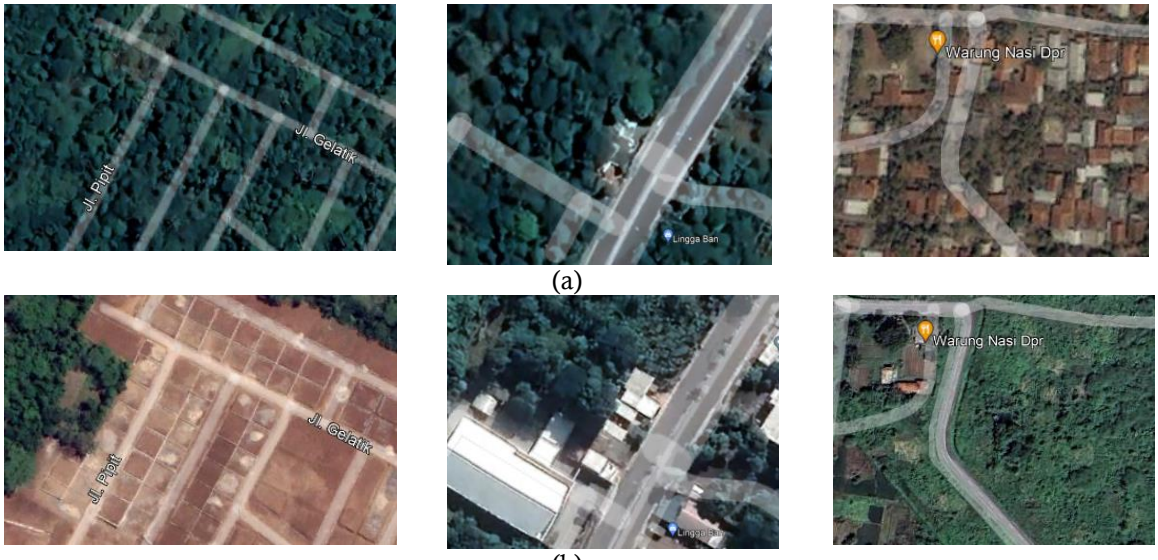

Figure 6. Illustration of Land Cover Around Kertajati International Airport, (a) Land cover in 2013, (b) Land cover in 2023, (Source: Google Earth Pro).

Based on Figure 6, the conversion of vegetation class to non-vegetation class is largely attributed to the development of residential areas and workplaces. Conversely, the transformation of non-vegetation to

E-ISSN: 2720-9326
P-ISSN: 2716-0459
DOI : 10.20885/EKSAKTA.vol6.iss1.art5

vegetation class, in some cases, involves the clearing of land for airport infrastructure within a certain radius. However, when compared with Table 7, the predominant change is from vegetation to non-vegetation class, primarily for the development of residential areas and small, medium, or large-scale industries. This phenomenon is driven by the airport's dual role—not only as an air transportation hub but also as a catalyst for regional economic development. The potential future economic value associated with the airport further reinforces this trend. These findings align with previous studies that highlight the role of airports as economic focal points [30], [31]. The tourism sector also benefits significantly from the presence of the airport, as it facilitates easier access for tourists to nearby destinations. This increase in tourist numbers positively impacts the hospitality and local transportation industries, while also boosting small and medium enterprises (SMEs) through the consumption of local products. Additionally, the airport contributes to infrastructure development, such as improved roads and lighting, both to and from the airport [32].

Conclusion

This study demonstrates that spatial classification using the Support Vector Machine (SVM) method successfully categorized land cover into two classes: vegetation and non-vegetation. After conducting four scenarios with multiple iterations and evaluating four types of kernels, the SVM with the Radial Basis Function (RBF) kernel was selected for land cover classification around Kertajati International Airport in Majalengka Regency, West Java Province. The selection of the RBF kernel was based on its superior average performance across five evaluation metrics: (1) accuracy, (2) specificity, (3) sensitivity, (4) f1-score, and (5) Area Under Curve (AUC). The evaluation metrics yielded satisfactory results, providing a reliable foundation for predicting land classes in the vicinity of the airport over time. The analysis revealed a decline in vegetation area from 2013 to 2023. Areas closer to the airport experienced more significant vegetation-to-non-vegetation changes compared to areas farther away. Most of the land cover changes were associated with the development of residential areas and businesses. However, further research is needed to quantify the economic impact of the airport's presence on the surrounding region.

Acknowledgment

The researchers extend their heartfelt gratitude to the Department of Statistics, Universitas Islam Indonesia, for their invaluable support, making this study possible. They hope the findings will serve as a meaningful contribution to those who may benefit from it.

References

[1] D. Setiady and P. Danoedoro, "Prediksi Perubahan Lahan Pertanian Sawah Sebagian Kabupaten Klaten dan Sekitarnya Menggunakan Cellular Automata dan Data Penginderaan Jauh," Universitas Gadjah Mada, Yogyakarta, 2016.

[2] I. Hanafi, Y. Pujowati, and M. A. Muhtadi, "Pengaruh Pembangunan Infrastruktur Transportasi Berkelanjutan terhadap Mobilitas dan Lingkungan di Kalimantan," *Jurnal Multidisiplin West Science*, vol. 02, no. 10, pp. 908–917, 2023.

[3] G. G. Praditya, "Hubungan Bandar Udara Kertajati dengan Perubahan Sosial-Ekonomi Penduduk Sekitar Bandara," 2021.

[4] A. Rahmadan *et al.*, "Dampak Pembangunan Bandara Internasional Jawa Barat Kertajati Terhadap Peningkatan Pendapatan Asli Daerah di Kabupaten Majalengka," *JURNAL PRINSIP VOLUME*, vol. 1, no. 1, 2024, doi: 10.36859/prinsip.v1i1.2929.

[5] B. Hermanto, "Dampak Pembangunan Bandara Internasional Kertajati dalam Kajian Green Political Theory," *Jurnal Ilmu Sosial dan Ilmu Politik Universitas Jambi (JISIP-UNJA)*, vol. 5, pp. 62–73, 2021.

[6] E. Transparan Putra Zebua and P. Rosyani, "Perancangan Deteksi Objek Kendaraan Bermotor Berbasis OpenCV Phyton menggunakan Metode HOG-SVM untuk Analisis Lalu Lintas Cerdas," *Jurnal Artificial Inteligent dan Sistem Penunjang Keputusan*, vol. 2, no. 1, pp. 16–26, 2024, [Online]. Available: https://jurnalmahasiswa.com/index.php/aidanspk

E-ISSN: 2720-9326
P-ISSN: 2716-0459
DOI : 10.20885/EKSAKTA.vol6.iss1.art5

[7] C. El Morr, M. Jammal, H. Ali-Hassan, and W. El-Hallak, "Support Vector Machine," 2022, pp. 385–411. doi: 10.1007/978-3-031-16990-8_13.
[8] S. Suthaharan, "Support Vector Machine," 2016, pp. 207–235. doi: 10.1007/978-1-4899-7641-3_9.
[9] M. A. Hearst, S. T. Dumais, E. Osuna, J. Platt, and B. Scholkopf, "Support vector machines," *IEEE Intelligent Systems and their Applications*, vol. 13, no. 4, pp. 18–28, 1998, doi: 10.1109/5254.708428.
[10] Y. Ma and G. Guo, Eds., *Support Vector Machines Applications*. Cham: Springer International Publishing, 2014. doi: 10.1007/978-3-319-02300-7.
[11] K. Saravanan, R. B. Prakash, C. Balakrishnan, G. V. P. Kumar, R. Siva Subramanian, and M. Anita, "Support Vector Machines: Unveiling the Power and Versatility of SVMs in Modern Machine Learning," in *2023 3rd International Conference on Innovative Mechanisms for Industry Applications (ICIMIA)*, 2023, pp. 680–687. doi: 10.1109/ICIMIA60377.2023.10426542.
[12] D. Anguita, A. Ghio, N. Greco, L. Oneto, and S. Ridella, "Model selection for support vector machines: Advantages and disadvantages of the Machine Learning Theory," in *The 2010 International Joint Conference on Neural Networks (IJCNN)*, 2010, pp. 1–8. doi: 10.1109/IJCNN.2010.5596450.
[13] G. W. Pereira, D. S. M. Valente, D. M. de Queiroz, N. T. Santos, and E. I. Fernandes-Filho, "Soil mapping for precision agriculture using support vector machines combined with inverse distance weighting," *Precis Agric*, vol. 23, no. 4, pp. 1189–1204, Aug. 2022, doi: 10.1007/s11119-022-09880-9.
[14] K. Ghanem, F. J. Aparicio-Navarro, K. G. Kyriakopoulos, S. Lambotharan, and J. A. Chambers, "Support Vector Machine for Network Intrusion and Cyber-Attack Detection," in *2017 Sensor Signal Processing for Defence Conference (SSPD)*, 2017, pp. 1–5. doi: 10.1109/SSPD.2017.8233268.
[15] J. and Z. S. A. and A. O. A. and L. M. and U. I. and I. C. Hai Tao and Zhou, "Evaluation of Text Classification Using Support Vector Machine Compare with Naive Bayes, Random Forest Decision Tree and K-NN," in *Proceedings of ICACTCE'23 — The International Conference on Advances in Communication Technology and Computer Engineering*, Z. and K. N. Iwendi Celestine and Boulouard, Ed., Cham: Springer Nature Switzerland, 2023, pp. 321–331.
[16] M. E. D. Chaves, M. C. A. Picoli, and I. D. Sanches, "Recent Applications of Landsat 8/OLI and Sentinel-2/MSI for Land Use and Land Cover Mapping: A Systematic Review," *Remote Sens (Basel)*, vol. 12, no. 18, p. 3062, Sep. 2020, doi: 10.3390/rs12183062.
[17] C. Wang *et al.*, "Landsat-8 to Sentinel-2 Satellite Imagery Super-Resolution-Based Multiscale Dilated Transformer Generative Adversarial Networks," *Remote Sens (Basel)*, vol. 15, no. 22, p. 5272, Nov. 2023, doi: 10.3390/rs15225272.
[18] Y. T. Widayati, Y. Prihati, and S. Widjaja, "Analisis dan Komparasi Algoritma Naive Bayes dan C4.5 untuk Klasifikasi Loyalitas Pelanggan MNC Play Kota Semarang," *TRANSFORMTIKA*, vol. 18, no. 2, pp. 161–172, 2021.
[19] S. F. Mohammed and G. J. M. Mahdi, "Non-linear support vector machine classification models using kernel tricks with applications," 2024, p. 040017. doi: 10.1063/5.0196147.
[20] A. Patle and D. S. Chouhan, "SVM kernel functions for classification," in *2013 International Conference on Advances in Technology and Engineering (ICATE)*, IEEE, Jan. 2013, pp. 1–9. doi: 10.1109/ICAdTE.2013.6524743.
[21] F. Putrawansyah, "Penerapan Metode Support Vector Machine Terhadap Klasifikasi Jenis Jambu Biji," *JIKO (Jurnal Informatika dan Komputer)*, vol. 8, no. 1, p. 193, Feb. 2024, doi: 10.26798/jiko.v8i1.988.
[22] R. Munawarah, O. Soesanto, M. Reza Faisal, J. A. Yani Km, and K. selatan, "Penerapan Metode Support Vector Machine Pada Diagnosa Hepatitis," *Kumpulan Jurnal Ilmu Komputer*, vol. 4, 2016.
[23] H.-C. Sun and Y.-C. Huang, "Support Vector Machine for Vibration Fault Classification of Steam Turbine-Generator Sets," *Procedia Eng*, vol. 24, pp. 38–42, 2011, doi: 10.1016/j.proeng.2011.11.2598.
[24] C. Z. V. Junus, T. Tarno, and P. Kartikasari, "Klasifikasi Menggunakan Metode Support Vector Machine dan Random Forest untuk Deteksi Awal Risiko Diabetes Melitus," *Jurnal Gaussian*, vol. 11, no. 3, pp. 386–396, Jan. 2023, doi: 10.14710/j.gauss.11.3.386-396.

E-ISSN: 2720-9326
P-ISSN: 2716-0459
DOI : 10.20885/EKSAKTA.vol6.iss1.art5

[25] L. Widya Astuti, I. Saluza, Faradilla, and M. Fadhiel Alie, "Optimalisasi Klasifikasi Kanker Payudara Menggunakan Forward Selection pada Naive Bayes," *Jurnal Ilmiah Informatika Global*, vol. 11, pp. 63–67, 2020, [Online]. Available: https://archive.ics.uci.edu/ml/machine-learning-

[26] G. M. Foody, "Challenges in the real world use of classification accuracy metrics: From recall and precision to the Matthews correlation coefficient," *PLoS One*, vol. 18, no. 10, p. e0291908, Oct. 2023, doi: 10.1371/journal.pone.0291908.

[27] P. Gimeno, V. Mingote, A. Ortega, A. Miguel, and E. Lleida, "Generalizing AUC Optimization to Multiclass Classification for Audio Segmentation With Limited Training Data," *IEEE Signal Process Lett*, vol. 28, pp. 1135–1139, 2021, doi: 10.1109/LSP.2021.3084501.

[28] S. Ruuska, W. Hämäläinen, S. Kajava, M. Mughal, P. Matilainen, and J. Mononen, "Evaluation of the confusion matrix method in the validation of an automated system for measuring feeding behaviour of cattle," *Behavioural Processes*, vol. 148, pp. 56–62, Mar. 2018, doi: 10.1016/j.beproc.2018.01.004.

[29] P. Rachman Hakim, A. Hadi Syafrudin, S. Salaswati, S. Utama, and W. Hasbi, "Development of Systematic Image Preprocessing of LAPAN-A3/IPB Multispectral Images," *International Journal of Advanced Studies in Computer Science in Engineering*, vol. 7, no. 10, 2018.

[30] S. Gibbons and W. Wu, "Airports, access and local economic performance: evidence from China," *J Econ Geogr*, vol. 20, no. 4, pp. 903–937, Jul. 2020, doi: 10.1093/jeg/lbz021.

[31] R. Florida, C. Mellander, and T. Holgersson, "Up in the air: the role of airports for regional economic development," *Ann Reg Sci*, vol. 54, no. 1, pp. 197–214, Jan. 2015, doi: 10.1007/s00168-014-0651-z.

[32] J. Cidell, "The role of major infrastructure in subregional economic development: an empirical study of airports and cities," *J Econ Geogr*, vol. 15, no. 6, pp. 1125–1144, Nov. 2015, doi: 10.1093/jeg/lbu029.